Dalton Transactions

PAPER

View Article Online
View Journal | View Issue

Cite this: *Dalton Trans.*, 2014, **43**, 10521

Preparation of layered double hydroxide/chlorophyll *a* hybrid nano-antennae: a key step†

Alicia E. Sommer Márquez,[a] Dan A. Lerner,*[b] Geolar Fetter,*[a] Pedro Bosch,[c] Didier Tichit[b] and Eduardo Palomares[d]

Received 13th January 2014,
Accepted 27th February 2014

DOI: 10.1039/c4dt00113c

www.rsc.org/dalton

In the first step to obtain an efficient nano-antenna in a bottom-up approach, new hybrid materials were synthesized using a set of layered double hydroxides (LDHs) with basic properties and pure chlorophyll *a* (Chl *a*). The stability of the adsorbed monolayer of Chl *a* was shown to be dependent on the nature and the ratio of the different metal ions present in the LDHs tested. The hybrid materials turned out to be adequate for stabilizing Chl *a* on Mg/Al LDHs for more than a month under ambient conditions while a limited catalytic decomposition was observed for the Ni/Al LDHs leading to the formation of pheophytin. These changes were followed by namely XRD, DR-UV-vis and fluorescence spectroscopies of the hybrid antennae and of the solutions obtained from their lixiviation with acetone or diethylether. On Mg/Al hydrotalcites the stability of the adsorbed Chl *a* was equivalent for values of the metal atom ratio ranging from 2 to 4. The latter hybrids should constitute a good basis to form efficient nanoscale light harvesting units following intercalation of selected dyes. This work describes an efficient preparation of Chl *a* that allows scale-up as well as the obtention of a stable Chl *a* monolayer on the surface of various LDHs.

Introduction

Chlorophylls are green pigments found in the chloroplasts of plants and algae as well as in cyanobacteria, in which they constitute a key component of the photosynthesis machinery. The basic structure of chlorophyll is that of a porphyrin ring (Scheme S1†) and its main function is to collect light from the sun. To this end, up to several hundreds of them are collectively organized as an antenna coupled to a trap. Resonant electronic energy transfer among members of the antenna occurs until the trap, known as the reaction center and constituted by a dedicated chlorophyll–protein complex, is reached. In the latter, the electronic energy is converted into chemical potential energy.[1,2] In these antennae, the chlorophylls are held in a fixed position by a strong interaction with specific peptides. However, although research in the field of artificial photosynthesis and molecular antennae produced an extensive literature, Chl *a* was seldom involved due to its overall instability.[3] As a consequence the most common strategy to obtain antenna-like systems used synthetic dyes adsorbed or immobilized on various supports. For instance Ru and Os polypyridyl complexes were introduced into a polymer.[4] Interesting aqueous soft matter based devices were also developed. For instance, spherical light gathering traps were obtained by self-assembly of alkylcobaloximes with various tensioactive molecules.[5] These coloured mixed micelles displayed bidimensional arrays of chromophores at their surface held in place by axial alkyl chains and revealed an original photochemistry.[6] A different type of aqueous soft matter based photovoltaic device using an anthracene derivative and $[Ru(bpy)_3]^{2+}$ was described by Koo *et al.*[7] and showed that solar cells that closely mimic nature could work effectively. However most of the recent work involved the presence of a solid support. As shown in the extensive work by the group of Calzaferri[8] a whole array of natural or synthetic dyes were adsorbed onto clays or zeolites. Porphyrins,[9] diazo dyes[10] or Ru(II)-polypyridine derivatives[11,12] were organized in LDH, saponite or nanoporous TiO_2 to form well-organized hybrid systems. The common benefit of these adsorptions and inclusions was the improved stability of the chromophoric molecules. Karlsson obtained a two-electron charge-separated state upon successive excitation by two photons.[12] In the same way, D.G. Nocera described a different and remarkable artificial leaf presented as a stand-alone device composed of earth-abundant materials (namely a Co cluster), providing a first step towards low-cost system engineering and manufacturing required for inexpensive solar-to-

[a]*Facultad de Ciencias Químicas, Universidad Autónoma de Puebla, Blvd. 14 Sur, 72570 Pueblo, PUE, Mexico*
[b]*Institut Charles Gerhardt, UMR 5253 CNRS, 8 rue Ecole Normale, 34296 Montpellier Cedex 5, France. E-mail: dan.lerner@enscm.fr*
[c]*Instituto de Investigaciones en Materiales, Universidad Nacional Autónoma de México, Circuito Exterior, C. U., 04510 México, D. F., Mexico*
[d]*Instituto de Tecnología Química (UPV-CSIC), Universidad Politécnica de Valencia, Av. de los Naranjos, 46022 Valencia, Spain*
†Electronic supplementary information (ESI) available. See DOI: 10.1039/c4dt00113c

fuel systems.[13] Noncovalent design principles have further addressed the processability of these hybrid light-harvesting systems. As noted by Venkata Rao, many hybrid systems have already shown promise in terms of energy-transfer efficiency and device applications.[14] Clearly, hybrids have advantages that cannot be achieved with single components as analyzed by G. Macchi.[15] Some of these, listed in his analysis of a bottom-up approach to materials for optoelectronics, are the structuring role of the matrix in the organization of the photoactive centers, the prevention of aggregation processes, and the potential for allowing a hierarchical organization.

However, in hybrid systems, it is known that any chlorophyll adsorbed or included in a solid possessing acidic centers would lose the Mg^{2+} atom and sometimes also the phytyl group.[16] So the acido–basic properties of an adsorbent should play a major role in the adsorption as well as in the stabilization of this adsorbate.[17–20] If Chl *a* is fragile, and has been seldom used in hybrids, the few examples found confirm however that its adsorption on solids results in some stabilization. This was the case with a smectite–Chl *a* association[19] or with Chl *a* adsorbed on a folded-sheet mesoporous silica,[21] which resulted in an enhancement of the photostability of Chl *a* and could photoreduce methyl viologen. In a different approach, a multiscale hybrid containing an oxygen-evolving photosynthetic reaction center complex (PSII) adsorbed into nanopores in SBA was able to display a high and stable activity of the photosynthetic oxygen-evolving reaction.[22]

LDHs are anionic exchangers whose acido–basic properties may be modulated depending on their composition, among others.[23,24] LDHs have the general formula: $[M^{2+}_{1-x}M^{3+}_{x}(OH)_2](A^{m-})_{x/m}\cdot nH_2O$, where M^{2+} is a divalent cation that may be substituted by trivalent M^{3+} cations, leaving positively charged layers with a brucite-like structure. This charge is neutralized by anions A^{m-}, such as CO_3^{2-}, SO_4^{2-}, NO_3^{-} *etc.*, situated in the interlayer space.[25–27] The nature and the ratio of the divalent to trivalent cations as well as the nature of the compensating anions determine several key properties of LDHs such as their anionic exchange capacity, their stability under different pH conditions, their specific surface area and their intrinsic acido–basicity. Overall, LDHs have a basic character.

In our laboratory, a bottom-up approach was adopted in view of assembling an efficient LDH-Chl *a* based hybrid system. The latter should allow visible light energy harvesting and conversion. In the present work, only one step of the assembly process is described and involves the study of the adsorption of a monolayer of pure Chl *a* on the external surface of various LDHs and of its stability in this adsorbed state. The project rests on the experience of the authors in the field of LDHs, including the intercalation of dyes (such as diazo dyes and copper chlorophyllins) between their brucite like layers,[10,28] and the photostability of conjugated molecules. The first step described here is considered to be a difficult one due to the fact that Chl *a* is a very fragile molecule. To obtain the final hybrid, LDHs intercalated with various selected auxiliary dyes will be prepared first. These intermediate hybrids will then be coated on their surface with Chl *a* to allow a more efficient photon harvesting and energy funneling to a photoactive trap.

All these elements strengthened our decision to work on a bottom-up approach to a new LDH-Chl *a* based hybrid system.

Experimental

Extraction, separation, and purification of Chl *a*

The leaves of fresh spinach were frozen at the liquid nitrogen temperature and immediately ground in an industrial mixer grinder. The resulting frozen flakes were extracted by cold ethanol (Aldrich 95%) in a thermostated ultrasonic bath and the supernatant was centrifuged and kept at 4 °C in light protected vessels. This solution contained a mixture of pigments. From this step onwards, all the work was carried out in a dark room under inactinic light and samples were covered with black cloth or aluminium foil. The separation of Chl *a* from the rest of the pigments was then carried out using a gravity fed flash dry chromatographic method. The latter was meant to quickly deliver a pure Chl *a*, free from Chl *b*, polyenes and xanthophylls, and in sizable amounts. A silica gel sorbent (high purity, pore size 60 Å, 63–200 μm, Fluka Analytical) was used on a specially made dismountable column (see materials and details of the separation in S2†). The solvents used were *n*-hexane (Carlo Erba 99.8%), petroleum ether (Carlo Erba 50–60), ethyl acetate (Aldrich 99.5%), acetone (Aldrich 99.5%), methanol (Aldrich 99.5%) and pure water (Milli-Q, Millipore Corp.).

Each flash chromatographic separation led to the obtention of about 60 mg of pure Chl *a* dissolved in pure ethanol. These concentrated solutions were used as stock solutions for the adsorption and spectroscopic studies. The amount of purified Chl *a* recovered after the chromatographic step was estimated to be about 1.5 g per kg from fresh spinach leaves, and the Chl *a*/Chl *b* ratio of the pure pigments was close to 3.2.

LDH synthesis

Two series of Mg/Al and Ni/Al LDHs were prepared. As nickel and magnesium differed in their electronegativity (1.8 and 1.2 respectively), a difference in the acido–basic properties of these LDHs was expected. The samples were prepared successively with a M^{2+}/Al^{3+} ratio of 2, 3 and 4 for Mg, and 2 and 3 for Ni, to vary the number of positive charges in the brucite-like layers (see S3† for details). In what follows these LDHs were denoted as M/Al(x), where M refers to the M^{2+} metal atom and x to the number ratio of the two metal atoms.

Adsorption of Chl *a* on LDH

In this section and in the following sections, only anhydrous solvents (exception 96% ethanol) were used to avoid the aggregation of Chl *a*. A small volume of the pure Chl *a* stock solution was diluted with 25 mL of acetone (or with 25 mL of diethylether) and put in contact with 500 mg of the chosen M/Al(x) LDH powder (previously dried for 24 h at 150 °C)

Table 1 Comparative UV-vis absorption and fluorescence data of interest (wavelengths in nm)

Sample	Soret band	Q_y band	F_{max}
Chl *a* (acetone)	430	662	669
Chl *a* (acetonitrile)	431	662	669
Chl *a* monolayer[a]	438	680	702
Mg/Al(2)-Chl	436	666	681
Mg/Al(3)-Chl	435	669	682
Mg/Al(4)-Chl	425	666	680
Chl *a* monolayer on smectite[b]	418	669	n.a.
Pheo *a* (acetone)	409	665.5	685

[a] Monolayer aggregates at the air–water interface at 0.98 nm^{-2} per molecule.[44] [b] Data from Ishii.[19]

added to a glass vial. The volume of stock solution taken with a digital pipette was selected, based on UV data, to contain the amount of Chl *a* necessary to form at least a single monolayer of Chl *a* on the surface of the resulting hybrid materials. This volume was estimated by taking into account the measured specific area of the LDH samples (Table 1) and the average value of the area of an adsorbed Chl *a* (~1.0 nm^2).[29,30] A set of samples with increasing concentrations was then tested and the amount of Chl *a* adsorbed was controlled until it reached the limit (the contact time was about 1 h 30 min). From there on the latter samples were left at room temperature in a fume cupboard in the dark until the solvent evaporated. To give an idea of the amounts involved, about 1.5×10^{-2} g Chl *a* is necessary to form a monolayer on 0.5 g of LDH having a specific area of 20 $m^2\ g^{-1}$.

Lixiviation of Chl *a* from the hybrid materials

In order to estimate the stability over time of Chl *a* adsorbed on the various hybrid materials, a solvent induced desorption of Chl *a* was carried out. For this purpose, 25 mg of the selected sample of the dried hybrid material kept in the dark for 3, 10 and 30 days were weighted and placed into a set of vials to which 2 mL of acetone or diethylether was added. The vials were immediately capped to limit the evaporation of the solvent and the samples were centrifuged at 5000 rpm (Eppendorf model 5804 R) at 20 °C for 15 min. The UV-Vis spectra of the supernatant were then recorded in 5 mm path length, stoppered quartz cells.

Characterization methods

CHNS-O elemental analyzer. The content of N, C and H in the samples was determined on a Fisons EA-1108 CHNS-O elemental analyzer.

Inductively coupled plasma (ICP). Al, Mg and Ni contents were measured by ICP-OES. The samples (*ca.* 20 mg), previously calcined, were dissolved in a HNO_3–HCl (1/3 vol.) solution before analysis with a Varian 715-ES ICP-Optical Emission Spectrometer.

X-ray diffraction (XRD). A Bruker-axs D8-advance diffractometer coupled to a copper anode X-ray tube was used to identify the crystalline compounds present in the powdered samples. A diffracted beam monochromator selected the K_α radiation.

Nitrogen adsorption. The BET surface areas were determined with a Micromeritics ASAP 2020 using the data from the nitrogen adsorption–desorption curves by the conventional multipoint technique. The pore size distribution curves were obtained by applying the BJH method to the desorption branch. The samples were pretreated at 150 °C for 12 hours under high vacuum.

Thermal analysis. Thermogravimetry and differential thermal analyses were performed on a Mettler Toledo TGA/SDTA 851 equipment, under air flow (50 $cm^3\ min^{-1}$). The sample weight was about 10 mg. The experiments were carried out in the range 25–800 °C at a heating rate of 10 °C min^{-1}. The weight change and the heat flow signal were continuously recorded for data processing.

DR-UV-vis spectroscopy. Diffuse reflectance ultraviolet spectra were obtained on a Perkin Elmer spectrometer Lambda 40. The spectra were scanned from λ = 800 nm down to 350 nm in quartz cells of 0.5 mm optical path, at a scan speed of 60 nm min^{-1}. The slit widths were set at 2 nm and the reference material was $BaSO_4$ (Aldrich, purity 99.998).

UV-Vis spectroscopy. Solution spectra were measured on a Perkin Elmer Lambda 35 spectrometer. Spectra were scanned from λ = 800 nm to 350 nm at a speed of 120 nm min^{-1} in 10 mm optical path quartz cells and the slit width was set at 2 nm.

Fluorescence spectroscopy. Steady-state fluorescence spectra were measured with a fluorimeter built around two Jobin Yvon M25 monochromators; each one fitted with continuously variable slits and a 1200 lines mm^{-1} grating (linear dispersion of 3 nm mm^{-1}). The source was a 150 W XBO short arc lamp (Osram) and the detector was a low noise R928 photomultiplier (Hamamatsu). The spectral bandwidth was set at 3 nm for both monochromators and the scanning speed was 50 nm mn^{-1}. All fluorescence spectra were recorded (uncorrected) under excitation at 430 nm. For emission spectra, Kodak filter types 3-70 or 3-71 were used.

All these spectroscopic measurements were performed in a dark room at 25 °C.

Results and discussion

LDH samples

Conventionally, LDH samples were synthesized by co-precipitation followed by a crystallization step at 80 °C for more than 18 hours.[31] To avoid lengthy crystallization time, microwave irradiation may be used[32–34] leading generally to a smaller crystallite size (see in S3†). Furthermore, microwave irradiation seemed to improve the distribution of the metal cations in the brucite-like layers.[35] For this basic synthesis the polydispersity of the particles is known to be large, from 20 nm to 200 nm for any batch.

X-ray diffraction. The XRD patterns of the Mg/Al(x) and Ni/Al(x) samples revealed that the latter were all crystalline (S4†) and identified as LDHs (JCPDS 41-1428).[36]

The lattice a parameter calculated from the position of the (110) peaks (Fig. S4†) at about 60° (2θ) ($a = 2 \times d_{110}$) decreased in both series of LDH when the M^{2+}/Al^{3+} molar ratio decreased (Table S5†). The a parameter indeed follows the Vegard's correlation when Mg^{2+} or Ni^{2+} is replaced by Al^{3+} of smaller ionic size in the brucite-like layers. The smaller ionic size of Ni^{2+} compared to Mg^{2+} also explained the lower a values observed in the Ni/Al(x) LDHs than in the corresponding Mg/Al(x) LDHs.

The elemental analyses (S5 and Table S5†) allowed establishing the structural formula of the samples.

Nitrogen physisorption. All isotherms corresponded to type IV in the IUPAC classification and were characteristic of mesoporous materials (Fig. S6a in S6†). The Mg/Al(x) LDH presented a H4 hysteresis loop associated with narrow slit mesopores formed between platelets as generally observed for layered materials.[37] The Ni/Al(x) LDHs presented hysteresis loops of H3 type in the IUPAC classification with any limiting adsorption at high P/P_0 associated with slit-shaped pores formed between rigid aggregates of plate-like particles.[38] The sizes of these mesopores were in the range from 3 to 7.5 nm (Fig. S6b†).

Thermal analysis. The TG-DTG curves of the samples were depicted in Fig. S7.† They exhibited the classical profile observed for LDHs with a weight loss in two steps.[39] It should be noted that the temperature of the second DTG peaks depended on the nature of the M^{2+} cation and on the Mg/Al ratio in the Mg/Al(x) samples (S7†). This temperature was representative of the bonding between the anions and the layers and it could be assumed, as previously shown by Sanchez *et al.*,[39,40] that it was correlated with the basicity of the samples. Therefore, our results were consistent with the decrease in basicity when going from the Ni/Al(x) to the Mg/Al(x) LDHs and in the latter series with the increase of the Mg/Al molar ratio.

Chl *a* extraction and characterization

The problem of the stability of Chl *a*. Solutions of the extracted Chl a were always known to be unstable and to quickly denature until 1997 when it was observed that freeze-drying of a solution of Chl could stabilize it as a powder allowing its use at a later stage. As a general rule, a decrease in Chl content was always observed with the increase of storage temperature and time.

The stability of chlorophylls has been analyzed following lyophilisation, controlled low-temperature vacuum dehydration or conservation in ultracold freezers (−80 to −90 °C), whether as pure pigments or in whole plants.[41] In a conventional freezer the onset of degradation of the pigments was observed only after 20 hours and degradation reached 5–10% after one to two months, whereas tests at −80 °C showed that the same amount of loss was obtained after one year.[42] It was then crucial in this work to see how the stability of Chl a would be affected by adsorption on selected solids chosen to be part of nano-antennae to use at a near ambient temperature. For these reasons it was deemed important to obtain a pure grade of Chl a in the shortest possible time (see S2 and Fig. S2†).

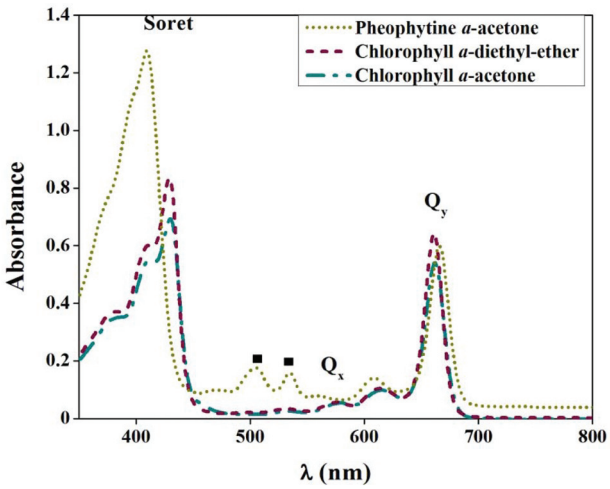

Fig. 1 UV-vis absorption spectra of Chl a in acetone and diethylether, and of Pheo a in acetone. The black squares point to the typical absorption bands of Pheo a.

UV-Vis absorption and fluorescence spectroscopies. In the visible range chlorophylls present two sets of absorption bands,[43] one in the blue region and one in the red region of the visible range. For Chl a dissolved in diethylether the two lowest-energy bands (Q bands) were observed at 662 nm (Q_y) and 578 nm (Q_x). A high-energy and more intense band (B or Soret band) was observed near 430 nm in diethylether. The absorption spectra of Chl a, purified as described above and dissolved in diethylether or acetone, are shown in Fig. 1, in perfect agreement with published data.

For comparison purposes the spectrum of pheophytin a (Pheo a) was also included as several degradation paths of Chl a begin with the formation of Pheo a (the structure and degradation path in Scheme S8†). The differences observed between Chl a and Pheo a spectra result from the loss of the metal ion (Mg^{2+}) present in the chlorin ring (Fig. 1) and are sufficiently important to easily discriminate the two compounds by means of UV-visible absorption spectroscopy, namely in the 500 to 550 nm region where typical new bands appear at 505 and 535 nm.

The fluorescence spectrum of Chl a is sensitive to the nature of the solvent. The maximum found at λ = 672 nm in acetone was shifted up to 678 nm in diethylether. For Pheo a in acetone, the fluorescence spectrum had its emission maximum at 685 nm (Fig. 2). Therefore, the two compounds can also be clearly distinguished by their emission spectra.

Adsorption on LDHs of Chl *a* dissolved in acetone or diethyl ether

X-ray diffraction. The XRD patterns of the dry materials obtained after treating Mg/Al(x) LDHs with an acetone solution

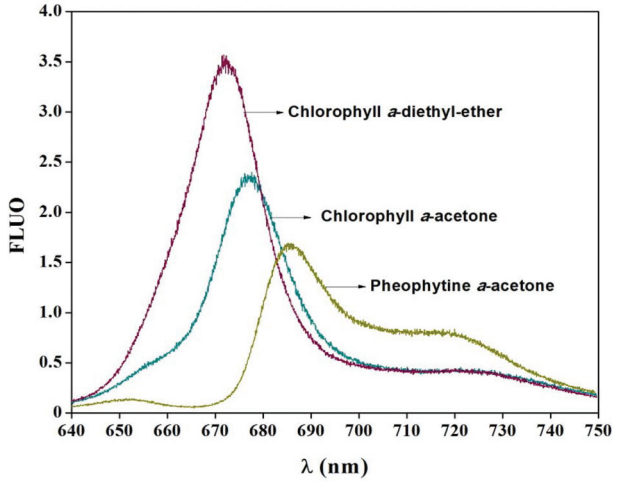

Fig. 2 Fluorescence spectra of Chl *a* in acetone and diethylether, and of Pheo *a* in acetone (λ_{ex} = 430 nm). Note that relative intensities are not meaningful here.

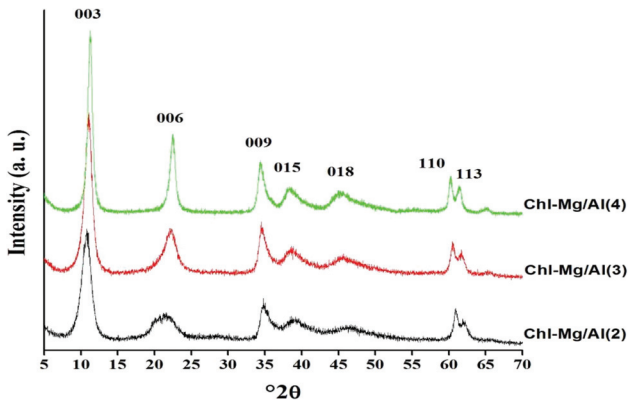

Fig. 3 XRD patterns of the Mg/Al(*x*)-Chl hybrids obtained with acetone.

of Chl *a* were compared (Fig. 3). In what follows these hybrid materials were denoted as M/Al(*x*)-Chl. All samples were crystalline and identified as LDHs.

Furthermore no crystalline compounds other than those reported previously for the as-prepared LDHs were observed (Fig. S4†). The interlamellar distance d_{003} was not affected by the adsorption of Chl *a*. Identical structures were obtained from ethyl ether solutions.

The XRD patterns of the Ni/Al(*x*) LDHs treated with Chl *a* dissolved in acetone gave similar results. These data showed that Chl *a* was not intercalated and was rather adsorbed on their external surface, independently of the composition and metal atom ratio of the LDHs. This was confirmed by the visual fading of the green color of the supernatant after centrifugation of the solids and by the greenish colour of the recovered solid. Actually the fact that no intercalation was observed was highly suspected as Chl *a* was both a neutral and very bulky species.

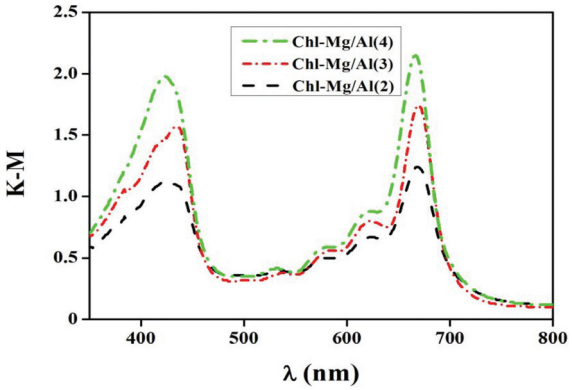

Fig. 4 DRS-UV-vis spectra of the Mg/Al(*x*)-Chl hybrids.

DR-UV-vis and fluorescence study of the hybrids

Mg/Al(x)-Chl samples. The following hybrids Mg/Al(2)-Chl, Mg/Al(3)-Chl and Mg/Al(4)-Chl were prepared as above, the chosen LDH being in contact with Chl *a* in acetone. In these freshly prepared hybrids, the Soret band, deduced from the UV reflectance spectra treated by the Kubelka–Munk transform, was respectively found at 426, 435 and 425 nm (Fig. 4). The Q_y bands appeared at 669 nm for Mg/Al(2)-Chl and Mg/Al(3)-Chl, and at 666 nm for Mg/Al(4)-Chl, respectively. At that stage these spectra clearly point to the presence of non-aggregated Chl *a* adsorbed on the solids, a proof that Chl *a* molecules can be successfully immobilized onto LDH particles without losing the Mg^{2+} ion in the process.

Interestingly, the Q_x bands of the Mg/Al(2)-Chl and Mg/Al(3)-Chl hybrids absorbed at the same wavelength as the first layer of Chl *a* deposited on smectite[19] although the surface properties of both minerals have a different nature. This feature could imply that molecules of water could participate in the adsorption of Chl *a* forming a bridge between its Mg^{2+} atom and the surface OH group of the LDHs or the surface oxygen atoms of smectite. The slight shifts in the DR-UV-vis spectra with respect to the solution were in agreement with the medium strength interaction between the organic and inorganic components of the hybrids. Furthermore the aspect ratio for the LDH platelets is high so that adsorption of Chl *a* must occur predominantly on the surface of the frontier brucite-like sheets.

Fluorescence spectra were similar to those of the Chl *a* molecule in solution, being only slightly bathochromically shifted due to the interaction between the solids and Chl *a*. The emission maxima were found at 681 nm for Mg/Al(2)-Chl, 682 nm for Mg/Al(3)-Chl, and 680 nm for Mg/Al(4)-Chl, with a vibronic component in the vicinity of 720 nm for all the hybrids (Fig. 5 and Table 1).

No difference was observed in the DR-UV-vis and fluorescence spectra of Mg/Al(*x*)-Chl hybrids obtained from Chl *a* previously either dissolved in diethylether or in acetone (Fig. S9†). Therefore, the nature of the solvent was not crucial for the preparation of these hybrid materials as long as it prevented the formation of aggregates.

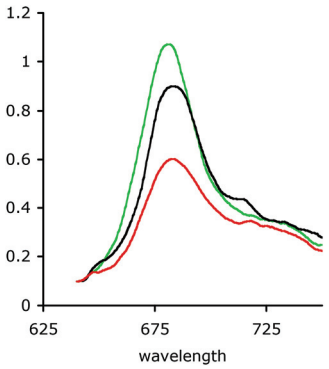

Fig. 5 Typical fluorescence spectra of typical Mg/Al(x)-Chl hybrids (λ_{ex} = 430 nm, black x = 2, red x = 3, green x = 4).

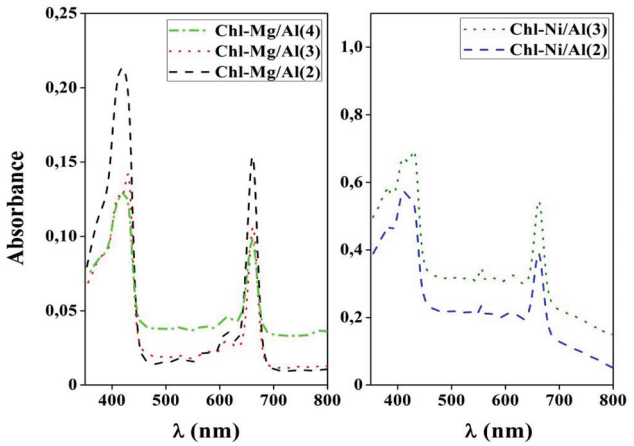

Fig. 6 UV-Vis absorption spectra of Chl *a* desorbed with acetone from Mg/Al(x)-Chl (left) and Ni/Al(x)-Chl (right) aged for 10 to 30 days. Some spectra are offset for the sake of clarity.

After periods varying from 3 to 30 days, lixiviation of Chl *a* from the surface of these hybrids with pure acetone (contact time of about 20 min) led to spectra of the desorbed pigment molecule typical of pure non-aggregated Chl *a* (Fig. 6 left). The Q_y band shifted back to 662 nm. The analysis of these spectra confirmed that Chl *a* was not altered when it remained adsorbed on LDHs. In some 30 day old samples, a small percentage of Pheo was observed amounting to about 0.5% of the total Chl *a* and two-month-old samples kept at 4 °C did not reveal any further evolution.

Ni/Al(x)-Chl samples. For these hybrids, the DR-UV-vis spectra only could be obtained as Ni atoms efficiently quenched the fluorescence of Chl *a* (Fig. 6). This feature seemed to indicate a very close proximity of the conjugated ring of Chl *a* to the Ni atoms of the superficial brucite-like layers of the LDHs. This was consistent with the hydrophilic nature of the superficial brucite-like layers that the long hydrophobic phytyl chains would try to avoid by orienting themselves away from the surface. All spectra were identical, irrespective of their Ni/Al molar ratio. If the Q_y band appeared at 670 nm, which reproduced the value found for Mg/Al(x)-Chl hybrids, after three days the Q_x band (578 nm, in Chl *a*) was no more visible. Perhaps more noteworthy is that both the Q_x and Soret bands of Chl *a* became much broader, a fact typical of aggregation of Chl *a* which occurred together with some partial degradation leading to the formation of Pheo *a*. Furthermore, some differences were observed in the spectra of samples prepared either from acetone or diethylether, the latter resulting in a faster degradation (Fig. S10†).

After periods varying from 3 to 30 days, these Ni/Al(x)-Chl hybrids were also lixiviated with acetone and the solutions were characterized by UV-vis spectroscopy (Fig. 6 right). All absorption band positions in the spectra were independent of the Ni/Al molar ratio. For Chl *a* they were all present but were weak, whereas bands at 380, 410, 503 and 535 nm belonging to Pheo *a* were more visible. A new peak appeared at 555 nm and had to be attributed to another unidentified Chl *a* decomposition species. So Chl *a* is efficiently decomposed on Ni/Al(x) LDHs. Therefore, the higher basicity of the Mg/Al(x)-Chl LDH clearly favours the stabilization of Chl *a*.

The lixiviating process run with diethyl ether led to identical conclusions. However the amount of pigment recovered was not so high with the latter solvent.

In the present work some of the expected properties of LDH were to play a role similar in some way to that of the peptidic scaffold in photosystem II by allowing the formation of a monolayer-like collection of ordered Chl *a* that would also protect those molecules against aggregation and decomposition. Considering that the cross-sectional area of the porphyrin plane is very close to 1 nm^2 (ref. 30) and taking into account the measured area of the LDHs, the dilution of the Chl *a* stock solution was initially estimated so that adsorption of the pigment would at least cover the nanoparticles of LDH with a single monolayer. After the adsorption step such solutions were partially depleted. More concentrated solutions were used afterwards (see the Experimental section) so that the solids adsorbed efficiently the natural pigment. But even for these latter samples, in absolute the solutions contained a relatively small amount of Chl *a*. Furthermore the DR-UV-vis spectra clearly showed the absence of interactions between the adsorbed Chl *a*, a feature that was hoped for but not expected at the outset. The spectroscopic analysis of the solvents used to recover the pigment after lixiviation of the hybrids also confirmed the presence of the non-aggregated form of Chl *a* only. So a monolayer like film covers the surface of these nanohybrids. This resulted probably from a stronger propensity of Chl *a* to bind to the surface OH groups of LDH *via* the Mg atom or *via* a bridging water molecule than to aggregate. This could be the leading parameter to explain the stabilization of Chl *a* observed. The various shifts in the absorption bands of Chl *a* in the different Mg/Al(x)-Chl hybrids revealed the presence of weak interactions that did not affect the stability of Chl *a*. The basic character of the Mg/Al(x) LDHs associated with their hydrophilic surface seems then to be the main factor leading to the formation of hybrids that remained stable for up to two months. In contrast, the less hydrophilic surface and lower basicity character due to the presence of the Ni atom in the

various Ni/Al(x)-Chl hybrids resulted in the quasi absence of stability of Chl *a* on these LDHs.

These results constitute an interesting step towards the future use of Chl *a* in artificial self-assembled nanosystems based on these types of hybrids.

Conclusion

Chlorophylls, including Chl *a*, are known to be very sensitive to temperature, low pH and UV-visible radiation. Their reactivity has strongly limited their use in artificial light collecting devices. In the present work Chl *a* was successfully immobilized onto the external surface of LDHs. It was shown that the stability of the adsorbed Chl *a* was strongly affected by the nature and the molar ratio of the cations in the LDHs, diminishing in the following sequence: Mg/Al(4) = Mg/Al(3) = Mg/Al(2) ≫ Ni/Al(2) = Ni/Al(3). For Mg/Al(x) lixiviating Chl *a* from the hybrid surface with two different solvents, acetone or diethylether, released molecular Chl *a* independently of the nature of the dry solvent. Furthermore, tests of lixiviation with acetone were carried out for ten and thirty days after the synthesis of the Mg/Al(x) hybrids and it was confirmed that even with an ageing time of minimum thirty days, the integrity of Chl *a* was maintained.

The first consequence of this feature is that these hybrids could be used to store Chl *a* after its purification, for up to two months under ambient conditions something that could not be done until now. Effectively the present methods which involve keeping Chl *a* under good conditions using liquid nitrogen or even ultra low temperature freezers is neither practical nor economical if integrated nano-systems containing Chl *a* were envisioned in the future. The present work intended to show that adsorption of Chl *a* on well-chosen solids could lead to a large increase in stability of the pigment at room temperature and in contact with air. This stabilization and the fact that Chl *a* was not aggregated even after its release warranted the multistep process required to prepare pure Chl *a*. This was recently comforted by initial tests carried out by the authors at the pilot scale allowing the preparation of batches of several tens of grams in one cycle.

The second consequence of the present work is that such hybrids seem fit to carry a further step in the bottom-up assembly of nanosystems as LDHs previously exchanged by intercalation with an anionic dye and eventually an added trap could allow a better light harvesting to prepare new integrated nanosystems. Work along these lines is already initiated and will include AFM analysis of the surface of these hybrids.

Acknowledgements

Thanks are due to Adriana Tejeda for the technical work in X-ray diffraction. The financial support from CONACYT (project 154060) is gratefully acknowledged.

References

1 R. E. Blankensip, *Molecular Mechanisms of Photosynthesis*, Blackwell Science Ltd, London, 2002.
2 D. Simpson and J. Knoetzel, in *Oxygenic Photosynthesis: the light reactions*, ed. D. O. a. C. Yocum, Kluwer, 1996, pp. 493–506.
3 A. F. Collings and C. Critchley, *Artificial Photosynthesis*, Wiley-VCH, Weinheim, 2005.
4 C. N. Fleming, K. A. Maxwell, J. M. DeSimone, T. J. Meyer and J. M. Papanikolas, *J. Am. Chem. Soc.*, 2001, **123**, 10366–10347.
5 D. A. Lerner, R. Ricchiero and C. Giannotti, *J. Colloid Interface Sci.*, 1979, **68**, 596–598.
6 D. A. Lerner, F. Ricchiero and C. Giannotti, *J. Phys. Chem.*, 1980, **84**, 3007–3011.
7 H.-J. Koo, S. T. Chang, J. M. Slocik, R. R. Naik and O. D. Velev, *J. Mater. Chem.*, 2011, **21**, 72–79.
8 G. Calzaferri and K. Lutkouskaya, *Photochem. Photobiol. Sci.*, 2008, **7**, 879–910.
9 J. Demel and K. Lang, *Eur. J. Inorg. Chem.*, 2012, 5154–5164.
10 S. Mandal, D. Tichit, D. A. Lerner and N. Marcotte, *Langmuir*, 2009, **24**, 9030–9037.
11 M. Ogawa, M. Sohmiya and Y. Watase, *Chem. Commun.*, 2011, **47**, 8602–8604.
12 S. Karlsson, J. Boixel, Y. Pellegrin, E. Blart, H. Becker, F. Odobel and L. Hammarström, *Faraday Discuss.*, 2012, **155**, 233–252; discussion 297–308.
13 D. G. Nocera, *Science*, 2011, 1209816.
14 K. V. Rao, K. K. R. Datta, M. Eswaramoorthy and S. J. George, *Chem.–Eur. J.*, 2012, **18**, 2184–2194.
15 G. Macchi, F. Meinardi, P. Valsesia and R. Tubino, *Int. J. Photoenergy*, 2008, 784691.
16 T. Watanabe, A. Hongu, K. Honda, M. Nakazato, M. Konno and S. Saitoh, *Anal. Chem.*, 1984, **56**, 251–256.
17 Y. Kodera, H. Kageyama and H. Sekine, *Biotechnol. Lett.*, 1992, **14**, 119–122.
18 R. Mokaya, W. Jones, M. E. Davis and M. E. Whittle, *J. Solid State Chem.*, 1994, **111**, 157.
19 A. Ishii, T. Itoh, H. Kageyama, T. Mizoguchi, Y. Kodera, A. Matsushima, K. Torii and Y. Inada, *Dyes Pigm.*, 1995, **28**, 77–82.
20 T. Itoh, A. Ishii, Y. Kodera, A. Matsushima, M. Hiroto, H. Nishimura, T. Tsuzuki, T. Kamachi, I. Okura and Y. Inada, *Bioconjugate Chem.*, 1998, **9**, 409–412.
21 T. Itoh, K. Yano, Y. Inada and Y. Fukushima, *J. Am. Chem. Soc.*, 2002, **124**, 13437–13441.
22 N. Tomoyasu, K. Chihiro, K. Keisuke, S. Jian-Ren, K. Tsutomu, F. Yoshiaki, S. Takeshi and I. Shigeru, *Langmuir*, 2011, **27**, 705–713.
23 A. Sampieri, G. Fetter, H. Pfeiffer and P. Bosch, *Solid State Sci.*, 2007, **9**, 394.
24 D. Tichit, A. Rolland, F. Prinetto, G. Fetter, M. J. Martínez-Ortíz, M. A. Valenzuela and P. Bosch, *J. Mater. Chem.*, 2002, **12**, 3832.

25 A. Alejandre, F. Medina, P. Salagre, X. Correig and J. E. Sueiras, *Chem. Mater.*, 1999, **11**, 939–948.
26 F. Cavani, F. Trifiro and A. Vaccari, *Catal. Today*, 1991, **11**, 173–301.
27 V. Rives and S. J. Kannan, *Mater. Chem.*, 2000, **10**, 489.
28 A. Sommer, A. Romero, G. Fetter, E. Palomares and P. Bosch, *Catal. Today*, 2013, **212**, 186–193.
29 Y. S. Nam, J. M. Kim, J.-W. Choi and W. H. Lee, *Mater. Sci. Eng.*, 2004, **C 24**, 35–38.
30 C. Chapados and R. M. Leblanc, *Biophys. Chem.*, 1983, **17**, 211–244.
31 J. He, M. Wei, B. Li, Y. Kang, D. G. Evans and X. Duan, *Struct. Bonding*, 2006, **119**, 89.
32 O. Bergada, P. Salagre, Y. Cesteros, F. Medina and J. E. Sueiras, *Adsorpt. Sci. Technol.*, 2007, **25**, 143–154.
33 P. Benito, F. M. Labajos and V. Rives, *Pure Appl. Chem.*, 2009, **81**, 1459–1471.
34 G. Fetter and P. Bosch, in *Pillared Clays and Related Catalysts*, ed. A. Gil, S. A. Korili, R. Trujillano and M. A. Vicente, Springer, New York, 2010, pp. 1–21.
35 M. Herrero, F. M. Labajos and V. Rives, *Appl. Clay Sci.*, 2009, **42**, 510.
36 W. Wong-Ng, H. F. McMurdie, C. R. Hubbard and A. D. Mighell, *J. Res. Natl. Inst. Stand. Technol.*, 2001, **106**(6), 1013–1028.
37 F. Rouquerol, J. Rouquerol and K. Sing, *Adsorption by Powders and Porous Solids: Principles, Methodology and Applications*, Academic Press, San Diego, 1999.
38 S. Lowell, J. E. Shields, M. A. Thomas and M. Thommes, *Characterization of porous solids and powders: surface area, pore size and density*, Kluwer Academic Publishers, Dordrecht, 2004.
39 *Layered Double Hydroxides: Present and Future*, ed. V. Rives, Nova Science Publishers, Inc., 2001.
40 J. Sanchez Valente, F. Figueras, M. Gravelle, P. Kumbhar, J. Lopez and J.-P. Besse, *J. Catal.*, 2000, **189**, 370–381.
41 V. A.-E. King, L. Chia-Fang and L. Yi-Jing, *Food Res. Int.*, 2011, **34**, 167–175.
42 *Introduction to marine phytoplankton and their pigments signatures*, ed. S. W. Jeffrey and M. Vesk, UNESCO Publishing, Paris, 1997.
43 G. Mackinney, *J. Biol. Chem.*, 1941, **140**, 315–322.
44 H. Heithier, K. Ballschmiter and H. Môhwald, *Photochem. Photobiol.*, 1983, **37**, 201–205.